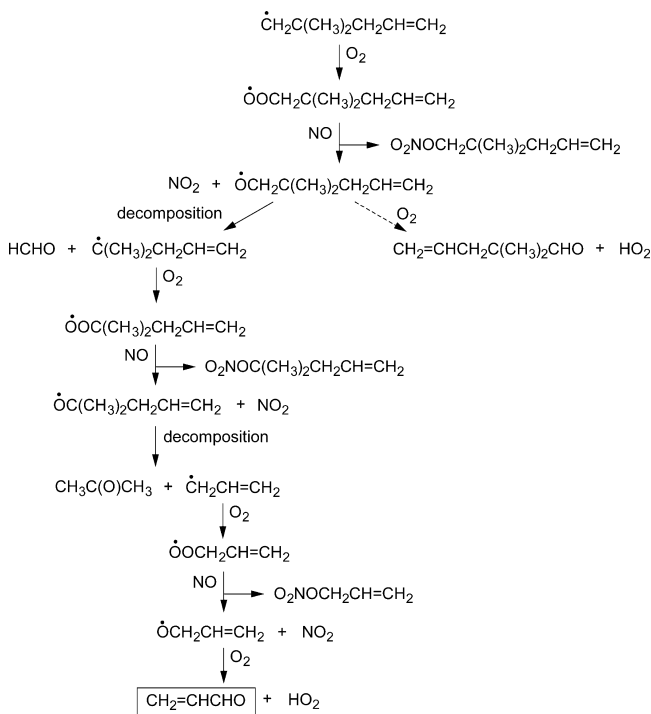
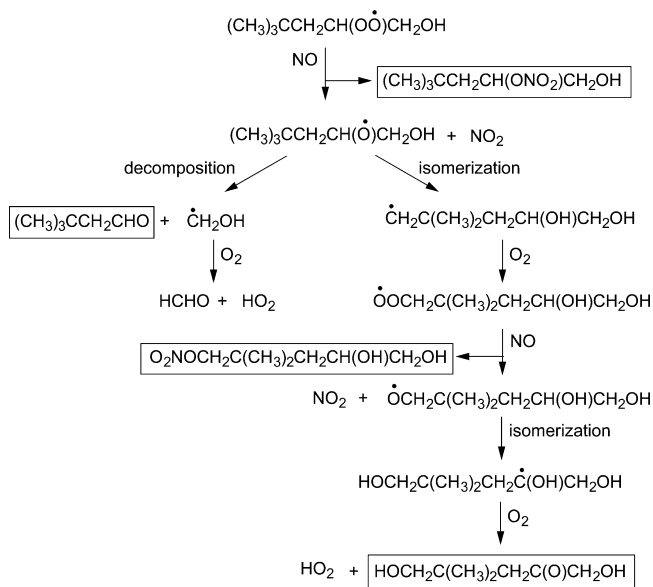


SCHEME 2: Expected Reactions of the Alkyl Radical Formed after H-Atom Abstraction from the Three Equivalent CH₃ Groups in 4,4-Dimethyl-1-pentene. Observed Product is Shown in Box. While Acetone was also Observed, it was Formed at Least in Part as a Second-Generation Product from OH + 3,3-Dimethylbutanal (see Scheme 5)

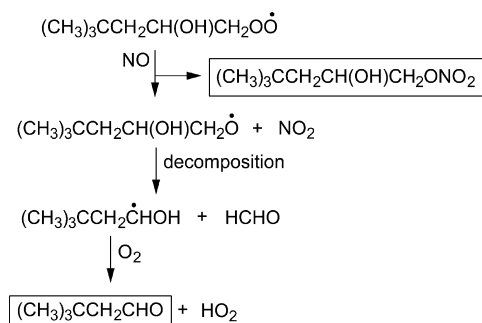


SCHEME 3: Expected Reactions of the Hydroxyalkyl Peroxy Radical Formed after OH Radical Addition at the 1-Position in 4,4-Dimethyl-1-pentene. Observed Products are Shown in Boxes

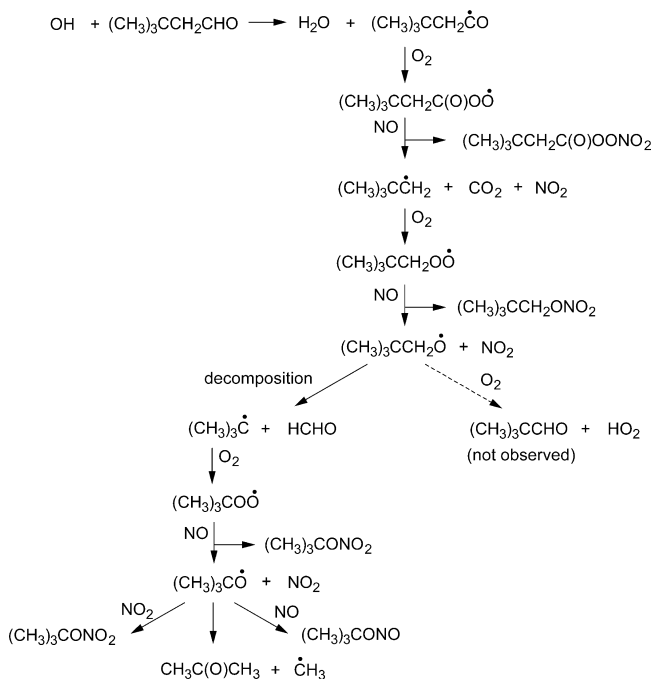


purified air. Both chambers are equipped with Teflon-coated fans to ensure rapid mixing of reactants during their introduction into the chamber, and one of the chambers is interfaced to a PE SCIEX API III MS/MS direct air sampling atmospheric pressure ionization mass spectrometer (API-MS).^{13,14} Hydroxyl radicals were generated by the photolysis of methyl nitrite (CH₃ONO) in the presence of O₂ at wavelengths >300 nm,^{13,14}

SCHEME 4: Expected Reactions of the Hydroxyalkyl Peroxy Radical Formed after OH Radical Addition at the 2-Position in 4,4-Dimethyl-1-pentene. Observed Products are Shown in Boxes

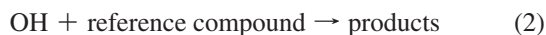


SCHEME 5: Expected Reactions after H-Atom Abstraction from the CHO Group in 3,3-Dimethylbutanal (The Expected Major Initial Reaction Pathway¹²)



and NO was included in the reactant mixtures to suppress the formation of O₃ and hence of NO₃ radicals.

Kinetic Studies. Rate constants for the reactions of OH radicals with 4,4-dimethyl-1-pentene and 3,3-dimethylbutanal were measured by a relative rate method in which the concentrations of the organic and a reference compound (whose OH radical reaction rate constant is reliably known) were measured in the presence of OH radicals:¹⁵



Providing that the organic and the reference compound reacted only with OH radicals then,¹⁵

$$\ln\left(\frac{[\text{organic}]_{t_0}}{[\text{organic}]_t}\right) = \frac{k_1}{k_2} \ln\left(\frac{[\text{reference compound}]_{t_0}}{[\text{reference compound}]_t}\right) \quad (I)$$

where $[\text{organic}]_0$ and $[\text{reference compound}]_0$ are the concentrations of the organic and reference compound, respectively, at time t_0 , $[\text{organic}]_t$ and $[\text{reference compound}]_t$ are the corresponding concentrations at time t , and k_1 and k_2 are the rate constants for reactions 1 and 2, respectively. The initial reactant concentrations (in molecules cm^{-3}) were: CH_3ONO and NO , $\sim 2.4 \times 10^{14}$ each; and that of organic and reference compounds $\sim 2.4 \times 10^{13}$ each. Methacrolein and, for experiments with 4,4-dimethyl-1-pentene, 1-octene were chosen as the reference compounds. Irradiations were carried out at 20% of the maximum light intensity for up to 15 min, resulting in up to 39 and 56% of the initially present 4,4-dimethyl-1-pentene and 3,3-dimethylbutanal, respectively, being consumed by reaction.

The concentrations of the organics and reference compounds were measured during the experiments by gas chromatography with flame ionization detection (GC-FID). For the analyses of 3,3-dimethylbutanal, methacrolein, 1-octene, and products (see below), gas samples of 100 cm^3 volume were collected from the chamber onto Tenax-TA adsorbent, with subsequent thermal desorption at ~ 250 °C onto a 30 m DB-1701 megabore column, initially held at -40 °C and then temperature programmed to 250 °C at 8 °C min^{-1} . Although 4,4-dimethyl-1-pentene could also be analyzed using this procedure, 4,4-dimethyl-1-pentene was incompletely collected onto the Tenax solid adsorbent and hence gas samples were collected from the chamber into a 100 cm^3 volume all-glass gastight syringe and transferred via a 1 cm^3 gas sampling loop onto a 30 m DB-5 megabore column initially held at -25 °C and then temperature programmed to 200 °C at 8 °C min^{-1} . Replicate analyses of 4,4-dimethyl-1-pentene, 3,3-dimethylbutanal, methacrolein, and 1-octene showed that the measurement uncertainties were typically $<3\%$.

Product Studies Using Gas Chromatography. Irradiations of $\text{CH}_3\text{ONO}/\text{NO}/4,4\text{-dimethyl-1-pentene}/\text{air}$ and $\text{CH}_3\text{ONO}/\text{NO}/3,3\text{-dimethylbutanal}/\text{air}$ mixtures were carried out with initial concentrations (molecules cm^{-3}) of CH_3ONO and NO , $\sim 2.4 \times 10^{13}$, $\sim 4.8 \times 10^{13}$ or $\sim 2.4 \times 10^{14}$ each (with the initial CH_3ONO and NO concentrations being equal in all experiments); and 4,4-dimethyl-1-pentene or 3,3-dimethylbutanal, $\sim 2.4 \times 10^{13}$. Analyses were carried out by GC-FID and combined gas chromatography–mass spectrometry (GC-MS). The GC-MS analyses were carried out using a DB-5 column (see below for details); the GC-FID analyses of 4,4-dimethyl-1-pentene and 3,3-dimethylbutanal and their products, collected onto Tenax solid adsorbent, were carried out using 30 m DB-1701 and DB-5 megabore columns with the temperature program noted above. The use of DB-5 columns for both the GC-MS and GC-FID analyses, together with *trans*-2-hexenal and *trans*-2-heptenal as additional retention time markers added to the chamber after the reaction, facilitated the identification of products from 4,4-dimethyl-1-pentene by providing an excellent linear correlation of retention times from the GC-MS and GC-FID analyses.

For the GC-MS analyses, samples from the chamber were collected onto Tenax solid adsorbent (100 or 500 cm^3 volume), onto a 65 μm polydimethylsiloxane/divinylbenzene (PDS/DVB) solid phase MicroExtraction (SPME) fiber exposed to the chamber contents for 10–60 min, or onto a PDS/DVB SPME fiber, precoated with *O*-(2,3,4,5,6-pentafluorobenzyl)hydroxylamine (PFBHA) for on-fiber derivatization of carbonyl compounds,¹⁶ and exposed to the chamber contents for 5 min. The Tenax solid adsorbent or SPME fibers were then thermally desorbed (injection port temperature at 250 °C) onto a 60 m DB-5MS capillary column (250 μm i.d., 0.25 μm phase) initially held at -50 °C (Tenax samples) or 40 °C (SPME samples) and

then temperature programmed, using an Agilent 6890N GC interfaced to an Agilent 5975 Inert XL Mass Selective Detector operated with methane as the reagent gas in positive ion mode (PCI-GC/MS) or in negative ion mode (NCI-GC/MS).

A sample was also collected from an irradiated $\text{CH}_3\text{ONO}/\text{NO}/4,4\text{-dimethyl-1-pentene}/\text{air}$ mixture through a 16.7 L min^{-1} , 2.5 μm Teflon-coated aluminum cyclone (URG-2000–30EH, UCR, Chapel Hill, NC) onto a 5-channel, 400 mm length denuder (URG-2000–30B5, URG, Chapel Hill, NC) coated with finely ground XAD-4 resin.¹⁷ Prior to sampling, the XAD-coated denuder was further coated with ~ 100 mg of PFBHA in 5 mL of methanol and then dried with a nitrogen gas flow.¹⁸ After sampling, the denuder was stored overnight and then extracted three times with 50 mL aliquots of CH_2Cl_2 (95% of the products were in the first extract). The extracts were rotoevaporated to a volume of ≤ 10 mL and then analyzed by PCI-GC/MS and NCI-GC/MS as described above. Note that each carbonyl group derivatized to an oxime added 195 mass units to the compound's molecular weight (MW), and methane-PCI gave characteristic protonated molecules ($[\text{M} + \text{H}]^+$) and smaller adduct ions at $[\text{M} + 29]^+$ and $[\text{M} + 41]^+$.^{18,19}

GC-FID response factors for 4,4-dimethyl-1-pentene, 3,3-dimethylbutanal, and acrolein were measured by introducing measured amounts of the chemicals into the chamber and then conducting several replicate analyses. The FID response factors for $(\text{CH}_3)_3\text{CCH}=\text{CHCHO}$ and the peaks that were assigned to hydroxynitrates were calculated using the effective carbon number (ECN)²⁰ of the products (5.9 for $(\text{CH}_3)_3\text{CCH}=\text{CHCHO}$), the measured GC-FID response factor for 3,3-dimethylbutanal, and the ECN of 3,3-dimethylbutanal (5.0).²⁰ For the hydroxynitrates, the ECNs were calculated using $\text{ECN}(-\text{CH}(\text{ONO}_2)-) = \text{ECN}(-\text{CH}_2\text{ONO}_2) = 0.2$ derived from measured GC-FID response factors for 3-methyl-2-butyl nitrate, 3-methyl-2-pentyl nitrate, 2-hexanone, and 3-methyl-2-pentanone.

Analyses by API-MS. Three $\text{CH}_3\text{ONO}/\text{NO}/4,4\text{-dimethyl-1-pentene}/\text{air}$ irradiations were carried out, during which the chamber contents were sampled through a 25 mm diameter by 75 cm length Pyrex tube at ~ 20 L min^{-1} directly into the API-MS source. The operation of the API-MS in the MS (scanning) and MS/MS [with collision activated dissociation (CAD)] modes has been described previously.^{13,14} Both positive and negative ion modes were used in this work. In positive ion mode, protonated water hydrates $(\text{H}_3\text{O}^+(\text{H}_2\text{O})_n)$ generated by the corona discharge in the chamber diluent air were responsible for the formation of protonated molecules ($[\text{M} + \text{H}]^+$), water adduct ions $[\text{M} + \text{H} + \text{H}_2\text{O}]^+$, and protonated homo- and heterodimers,¹³ whereas in negative ion mode O_2^- , NO_2^- and NO_3^- ions were responsible for formation of adduct ions.¹⁴

The initial concentrations (molecules cm^{-3}) were: CH_3ONO , NO , and 4,4-dimethyl-1-pentene, $\sim 2.4 \times 10^{13}$ each. The reactant mixtures were irradiated for 3–8.3 min at 20% of the maximum light intensity.

Chemicals. The chemicals used, and their stated purities, were: acrolein (90%), 3,3-dimethylbutanal (95%), 4,4-dimethyl-1-pentene (99%), 2,2-dimethylpropanal [trimethylacetaldehyde] (97%), *trans*-2-hexenal (98%), *trans*-2-heptenal (97%), and methacrolein (95%), Aldrich; 1-octene (99.9%), ChemSampCo; 1-octene (99.0%), TCI America; acetone (HPLC grade), Fisher Scientific; and NO (99.0%), Matheson Gas Company. Methyl nitrite was prepared as described by Taylor et al.²¹ and stored at 77 K under vacuum.

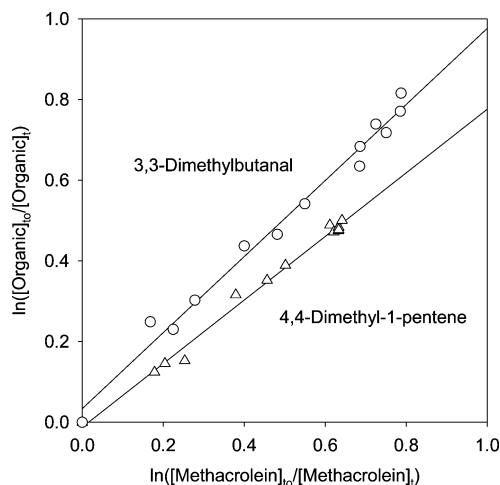


Figure 1. Plots of eq I for the reactions of OH radicals with 4,4-dimethyl-1-pentene and 3,3-dimethylbutanal, with methacrolein as the reference compound. GC-FID analyses of 3,3-dimethylbutanal and methacrolein by thermal desorption of samples collected onto Tenax solid adsorbent onto a 30 m DB-1701 column; GC-FID analyses of 4,4-dimethyl-1-pentene used the syringe/gas sampling loop procedure and a 30 m DB-5 column.

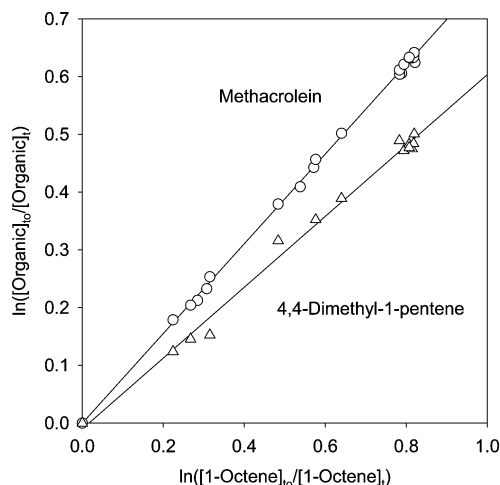


Figure 2. Plots of eq I for the reactions of OH radicals with 4,4-dimethyl-1-pentene and methacrolein, with 1-octene as the reference compound. GC-FID analyses of methacrolein and 1-octene by thermal desorption of samples collected onto Tenax solid adsorbent onto a 30 m DB-1701 column; GC-FID analyses of 4,4-dimethyl-1-pentene used the syringe/gas sampling loop procedure and a 30 m DB-5 column.

Results

Rate Constants for OH + 4,4-Dimethyl-1-pentene and 3,3-Dimethylbutanal. The experimental data from $\text{CH}_3\text{ONO}/\text{NO}/\text{air}$ irradiations of 4,4-dimethyl-1-pentene + methacrolein + 1-octene and 3,3-dimethylbutanal + methacrolein mixtures are plotted in accordance with eq I in Figures 1 and 2. The rate constant ratios k_1/k_2 obtained from least-squares analyses of these data are listed in Table 1 and are placed on an absolute basis using rate constants of $k_2(\text{methacrolein}) = 2.89 \times 10^{-11} \text{ cm}^3 \text{ molecule}^{-1}$ at 296 K^{5,22} and $k_2(1\text{-octene}) = 4.14 \times 10^{-11} \text{ cm}^3 \text{ molecule}^{-1}$ at $295 \pm 1 \text{ K}$.²³ Since both methacrolein and 1-octene were used as reference compounds for 4,4-dimethyl-1-pentene and were present in the same reactant mixtures, a rate constant ratio $k(\text{OH} + \text{methacrolein})/k(\text{OH} + 1\text{-octene})$ was also obtained. Our measured rate constant ratio $k(\text{OH} + \text{methacrolein})/k(\text{OH} + 1\text{-octene}) = 0.777 \pm 0.011$ (where the indicated error is two least-squares standard deviations) is in

good agreement with that of 0.698 derived from the recommended 296 K rate constant for methacrolein^{5,22} and the rate constant at $295 \pm 1 \text{ K}$ for 1-octene recently measured in our laboratory.²³

Products of OH + 4,4-Dimethyl-1-pentene. Analyses by Gas Chromatography. GC-FID analyses of irradiated $\text{CH}_3\text{ONO}/\text{NO}/4,4\text{-dimethyl-1-pentene}/\text{air}$ and $\text{CH}_3\text{ONO}/\text{NO}/3,3\text{-dimethylbutanal}/\text{air}$ mixtures showed that many of the GC peaks observed in the $\text{CH}_3\text{ONO}/\text{NO}/4,4\text{-dimethyl-1-pentene}/\text{air}$ irradiations were due to secondary formation from OH + 3,3-dimethylbutanal. In addition to GC-FID analyses of authentic standards of acrolein, acetone, 4,4-dimethyl-1-pentene, 3,3-dimethylbutanal, and 2,2-dimethylpropanal introduced into the chamber, GC-FID analysis of an irradiated $\text{CH}_3\text{ONO}/\text{NO}/2\text{-methylpropane}/\text{air}$ mixture was also carried out. The OH radical-initiated reaction of 2-methylpropane leads to formation of $(\text{CH}_3)_3\text{C}^\bullet$ radicals and hence to acetone, *tert*-butyl nitrite, and *tert*-butyl nitrate,^{4,5} and this analysis aided in the peak assignments. As expected (see Scheme 5), the OH + 3,3-dimethylbutanal reaction led to the formation of acetone, *tert*-butyl nitrite, and *tert*-butyl nitrate (and methyl nitrate from photooxidation of CH_3ONO), but with no observable amount of 2,2-dimethylpropanal.²⁴

Products identified as arising uniquely from the OH + 4,4-dimethyl-1-pentene reaction were 3,3-dimethylbutanal, acrolein, and a MW 112 product attributed to $(\text{CH}_3)_3\text{CCH}=\text{CHCHO}$. 3,3-Dimethylbutanal was identified by retention time and mass spectral matching of samples collected onto Tenax solid adsorbent, PFBHA-coated SPME fibers, and the PFBHA-coated XAD-denuder with those of an authentic standard similarly sampled. Acrolein was identified by retention time and mass spectral matching of a sample collected onto the PFBHA-coated XAD-denuder and from retention time matching in the GC-FID analyses, and the MW 112 carbonyl attributed to $(\text{CH}_3)_3\text{CCH}=\text{CHCHO}$ was observed from GC-MS analyses of samples collected onto Tenax solid adsorbent and the PFBHA-coated XAD-denuder (see footnotes to Table 2 for details). Unfortunately, attempts to have $(\text{CH}_3)_3\text{CCH}=\text{CHCHO}$ and its possible precursor (from OH radical- or O_3 -initiated reactions) $(\text{CH}_3)_3\text{CCH}=\text{CHCH}=\text{CH}_2$ synthesized by commercial laboratories were unsuccessful.

Acrolein, 3,3-dimethylbutanal and $(\text{CH}_3)_3\text{CCH}=\text{CHCHO}$ react with OH radicals, hence their measured concentrations were corrected for reaction with OH radicals as described previously,²⁵ using rate constants (in units of $10^{-11} \text{ cm}^3 \text{ molecule}^{-1} \text{ s}^{-1}$) of: 4,4-dimethyl-1-pentene, 2.28 (relative to methacrolein); acrolein, 1.99;²⁶ 3,3-dimethylbutanal, 2.73; and $(\text{CH}_3)_3\text{CCH}=\text{CHCHO}$, 3.9 (estimated¹² and similar to the rate constant for OH + crotonaldehyde²⁶). The multiplicative factors to account for secondary reactions increase with $k(\text{OH} + \text{product})/k(\text{OH} + 4,4\text{-dimethyl-1-pentene})$ and with the extent of reaction²⁵ and were ≤ 1.28 for acrolein, ≤ 1.55 for 3,3-dimethylbutanal, and ≤ 1.59 for $(\text{CH}_3)_3\text{CCH}=\text{CHCHO}$, with $\pm 10\%$ uncertainties in the rate constant ratios $k(\text{OH} + \text{product})/k(\text{OH} + 4,4\text{-dimethyl-1-pentene})$ leading to $< 5\%$ uncertainties in the maximum values of the multiplicative correction factors.

Figure 3 shows a plot of the amounts of 3,3-dimethylbutanal formed, corrected for reaction with OH radicals, against the amounts of 4,4-dimethyl-1-pentene reacted, and Figure 4 shows analogous plots for formation of acrolein and $(\text{CH}_3)_3\text{CCH}=\text{CHCHO}$. Data for 3,3-dimethylbutanal in Figure 3 are from two independent sets of experiments with analyses of 3,3-dimethylbutanal using a DB-1701 GC column and a DB-5 GC column, with separate calibrations of 4,4-dimethyl-1-pentene

TABLE 1: Rate Constant Ratios k_1/k_2 and Rate Constants k_1 at 296 ± 2 K and Atmospheric Pressure of Air

organic	reference compound	k_1/k_2^a	$10^{11} \times k_1$ (cm ³ molecule ⁻¹ s ⁻¹) ^b
4,4-dimethyl-1-pentene	methacrolein	0.788 ± 0.041	2.28 ± 0.12
4,4-dimethyl-1-pentene	1-octene	0.614 ± 0.031	2.54 ± 0.13
3,3-dimethylbutanal	methacrolein	0.943 ± 0.068	2.73 ± 0.20
methacrolein	1-octene	0.777 ± 0.011	3.22 ± 0.05

^a Indicated errors are two least-squares standard deviations. ^b Placed on an absolute basis using $k_2(\text{OH} + \text{methacrolein}) = 2.89 \times 10^{-11}$ cm³ molecule⁻¹ at 296 K^{5,22} and $k_2(\text{OH} + 1\text{-octene}) = 4.14 \times 10^{-11}$ cm³ molecule⁻¹ at 295 \pm 1 K.²³ Indicated errors are two least-squares standard deviations and do not take into account the uncertainties in the rate constants k_2 (see text).

TABLE 2: Observed Products of the Reaction of OH Radicals with 4,4-Dimethyl-1-pentene in the Presence of NO

product	analysis by		
	Tenax GC-FID ^a	GC-MS	API-MS
3,3-dimethylbutanal (MW 100) (CH ₃) ₃ CCH ₂ CHO	59 ± 6^b	confirmed with standard	observed ^c
acrolein (MW 56) CH ₂ =CHCHO	2.7 ± 0.5^d	confirmed with standard	
4,4-dimethyl-2-pentenal (MW 112) (CH ₃) ₃ CCH=CHCHO	3.4 ± 0.6^d	aldehyde of MW 112 ^e	observed ^f
MW 177 hydroxynitrates (CH ₃) ₃ CCH ₂ CH(OH)CH ₂ ONO ₂ and/or (CH ₃) ₃ CCH ₂ CH(ONO ₂)CH ₂ OH	$\sim 15^g$	PCI and NCI consistent with hydroxynitrate of MW 177 ^h	observed ⁱ
MW 146 dihydroxycarbonyl HOCH ₂ C(CH ₃) ₂ CH ₂ C(O)CH ₂ OH			observed ^j
MW 193 dihydroxynitrate O ₂ NOCH ₂ C(CH ₃) ₂ CH ₂ CH(OH)CH ₂ OH			observed ^k

^a Indicated errors are two least-squares standard deviations (from plots such as those shown in Figures 3 and 4) combined with estimated overall uncertainties in the GC-FID response factors of $\pm 5\%$ for 4,4-dimethyl-1-pentene, 3,3-dimethylbutanal, and acrolein and $\pm 15\%$ for the response factor of (CH₃)₃CCH=CHCHO relative to that measured for 3,3-dimethylbutanal. ^b Formation yield of $58 \pm 6\%$ from experiments with GC-FID analysis of 3,3-dimethylbutanal using a DB-1701 column, and $60 \pm 6\%$ from experiments with GC-FID analysis of 3,3-dimethylbutanal using a DB-5 column. ^c Observed in positive ion mode from ion peaks at 101 u [100 + H]⁺, 119 u [100 + H₂O + H]⁺, 159 u [100 + 58 + H]⁺, 201 u [100 + 100 + H]⁺, 213 u [100 + 112 + H]⁺ and 278 u [100 + 177 + H]⁺, where the MW 58 species is attributed to acetone formed from 4,4-dimethyl-1-pentene (minor) and 3,3-dimethylbutanal. ^d Data from experiments with GC-FID analyses of acrolein and (CH₃)₃CCH=CHCHO using a DB-5 column. Formation yield of $2.9 \pm 0.5\%$ derived from GC peak attributed to (CH₃)₃CCH=CHCHO in experiments with GC-FID analyses using a DB-1701 column (see text). ^e [M + H]⁺ of 113 u observed in Tenax GC-MS PCI analysis. [M + H]⁺ of oxime derivative observed at 308 u in GC-MS analysis of denuder extract and small 239 u fragment consistent with a derivatized aldehyde of MW 112. ^f Observed in positive ion mode from ion peaks at 171 u [112 + 58 + H]⁺, 213 u [100 + 112 + H]⁺ and 225 u [112 + 112 + H]⁺, where the MW 58 species is attributed to acetone formed from 4,4-dimethyl-1-pentene (minor) and 3,3-dimethylbutanal. ^g Two peaks tentatively identified as 1,2-hydroxynitrates were observed in Tenax samples and in denuder samples analyzed with cool on-column injection (but not seen in SPME samples or denuder extracts analyzed with splitless injection). Quantification based on estimated ECNs (see text) results in formation yields of the two 1,2-hydroxynitrates of 4.4% and 10.9%, which should strictly be considered as lower limits because of potential losses during the GC analyses. ^h No molecular ions observed in PCI analysis; both peaks gave a 115 u fragment ion attributed to [M + H - HNO₃]⁺ and a small 160 u fragment ion attributed to [M + H - H₂O]⁺. In NCI mode, [NO₂]⁻ at 46 u was a strong fragment ion and ion peaks at 129 u and 131 u were attributed²⁷ to [M - NO₂ - 2H]⁻ and [M - NO₂]⁻, respectively, of MW 177 1,2-hydroxynitrates. ⁱ Observed in positive ion mode from ion peak at 278 u [100 + 177 + H]⁺, and in negative ion mode from ion peaks at 209 u [177 + O₂]⁻, 223 u [177 + NO₂]⁻, 239 u [177 + NO₃]⁻ (see also footnote k below) and 400 u [177 + 177 + NO₂]⁻. ^j Observed in positive ion mode from ion peak at 129 u [146 + H - H₂O]⁺, and in negative ion mode from ion peak at 192 u [146 + NO₂]⁻. ^k Observed in negative ion mode from ion peak at 225 u [193 + O₂]⁻. Note that the 239 u ion peak could be [177 + NO₃]⁻ and/or [193 + NO₂]⁻.

and 3,3-dimethylbutanal for each set of experiments. Least squares analyses of the two sets of data result in formation yields of 3,3-dimethylbutanal of $58 \pm 6\%$ (DB-1701 column) and $60 \pm 6\%$ (DB-5 column), respectively, where the indicated errors are the two least-squares standard deviations combined with estimated uncertainties in the GC-FID response factors for 4,4-dimethyl-1-pentene and 3,3-dimethylbutanal of $\pm 5\%$ each. The agreement is excellent, with an average 3,3-dimethylbutanal formation yield of $59 \pm 6\%$. The data shown in Figure 4 for acrolein and (CH₃)₃CCH=CHCHO are from experiments with analyses using the DB-5 column. On this GC column, acrolein was significantly better resolved from acetone (but still not completely baseline resolved) than on the DB-1701 column. As noted above, the MW 112 product attributed to (CH₃)₃CCH=CHCHO identified by GC-MS analyses on a DB-5 column could be confidently assigned on the DB-5 column used for the GC-FID analyses from the excellent linear correlation of retention times from the GC-MS and GC-FID analyses. A

GC peak on the GC-FID analyses using the DB-1701 column was assigned, with less confidence, to (CH₃)₃CCH=CHCHO, resulting in a formation yield of $2.9 \pm 0.5\%$, essentially identical to that of $3.4 \pm 0.6\%$ for the data presented in Figure 4 from the use of the DB-5 column.

Two other products were observed from the Tenax analyses of the OH + 4,4-dimethyl-1-pentene reaction and they exhibited intense 46 u fragment ions in their NCI-GC/MS analyses, and hence are likely to be nitrates.²⁷ In the denuder extracts, these peaks were only seen when cool on-column injection was utilized, suggesting thermal decomposition and/or irreversible adsorption in the hot injector when using the splitless mode. This behavior is consistent with that reported for 1,2-hydroxynitrates by Muthuramu et al.²⁸ On the basis of the PCI and NCI mass spectra (see footnotes g and h in Table 2 for details), we attribute these to the MW 177 hydroxynitrates (CH₃)₃CCH₂CH(OH)CH₂ONO₂ and (CH₃)₃CCH₂CH(ONO₂)CH₂OH (see Schemes 3 and 4). Because the estimated rate

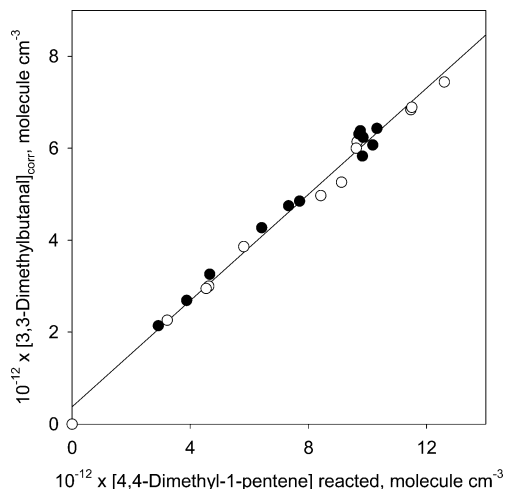


Figure 3. Plot of the amounts of 3,3-dimethylbutanal formed, corrected for reaction with OH radicals (see text), against the amounts of 4,4-dimethyl-1-pentene reacted. GC-FID analyses of 3,3-dimethylbutanal by thermal desorption of samples collected onto Tenax solid adsorbent using: O, a 30 m DB-1701 column; ●, a 30 m DB-5 column. In all cases, GC-FID analyses of 4,4-dimethyl-1-pentene used the syringe/gas sampling loop procedure and a 30 m DB-5 column. The solid line is a least-squares fit to the combined data set.

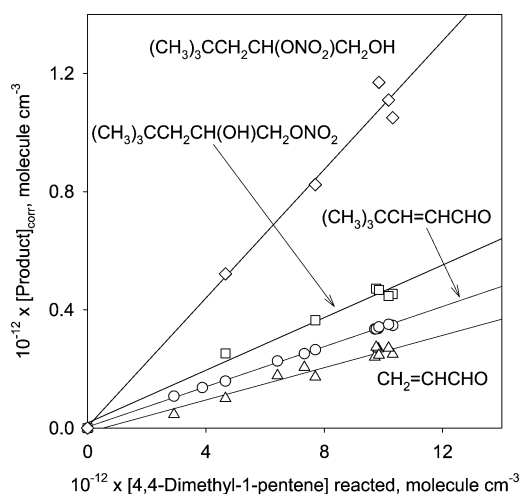


Figure 4. Plots of the amounts of acrolein, 4,4-dimethyl-2-pentenal, and the two 1,2-hydroxynitrates (attributed to $(\text{CH}_3)_3\text{CCH}_2\text{CH}(\text{ONO}_2)\text{CH}_2\text{OH}$ and $(\text{CH}_3)_3\text{CCH}_2\text{CH}(\text{OH})\text{CH}_2\text{ONO}_2$) formed against the amounts of 4,4-dimethyl-1-pentene reacted. The measured concentrations of acrolein and 4,4-dimethyl-2-pentenal have been corrected for reaction with OH radicals (see text). GC-FID analyses of acrolein, 4,4-dimethyl-2-pentenal, and the 1,2-hydroxynitrates by thermal desorption of samples collected onto Tenax solid adsorbent using a 30 m DB-5 column; GC-FID analyses of 4,4-dimethyl-1-pentene used the syringe/gas sampling loop procedure and a 30 m DB-5 column.

constants for reactions of OH radicals with $(\text{CH}_3)_3\text{CCH}_2\text{CH}(\text{OH})\text{CH}_2\text{ONO}_2$ and $(\text{CH}_3)_3\text{CCH}_2\text{CH}(\text{ONO}_2)\text{CH}_2\text{OH}$ are 5.9×10^{-12} and $2.6 \times 10^{-12} \text{ cm}^3 \text{ molecule}^{-1} \text{ s}^{-1}$, respectively,²⁹ corrections for secondary reactions were minor (<8%) and were neglected. Assuming that these two GC-FID peaks were the C₇-hydroxynitrates, then their formation yields were 4.4 and 10.9%, and since OH radical addition to the terminal carbon is expected to dominate,⁵ these yields would be for $(\text{CH}_3)_3\text{CCH}_2\text{CH}(\text{OH})\text{CH}_2\text{ONO}_2$ and $(\text{CH}_3)_3\text{CCH}_2\text{CH}(\text{ONO}_2)\text{CH}_2\text{OH}$, respectively. The sum of the hydroxynitrate formation yields of ~15% is a factor of ~2 higher than expected based on the yield data of O'Brien et al.³⁰ for hydroxynitrate formation from a series of C₂–C₆ alkenes and is about the

same as the hydroxynitrate yields measured from C₁₄–C₁₇ alkenes ($14.0 \pm 0.9\%$) by Matsunaga and Ziemann.³¹

Analyses by API-MS. API-MS analyses of irradiated CH₃ONO/NO/4,4-dimethyl-1-pentene/air mixtures were carried out in both positive and negative ion modes. In positive ion mode, the API-MS spectrum was dominated by ion peaks at 119, 129, and 201 u, with less intense peaks at 101, 159, 171, 213, 225, and 278 u. API-MS/MS product ion spectra showed these ion peaks to be due to products of MW 58, 100, 112, 146, and 177 (see Table 2). In negative ion mode, the API-MS was dominated by peaks at 223, 239, and 400 u, with less intense ion peaks at 192, 209, and 225 u, with API-MS/MS product ion spectra showing these to be due to products of MW 146, 177, and 193 u (Table 2).

Discussion

Our rate constant for 3,3-dimethylbutanal ($2.73 \times 10^{-11} \text{ molecule}^{-1} \text{ s}^{-1}$) is a factor of 1.3 higher than that of $2.14 \times 10^{-11} \text{ molecule}^{-1} \text{ s}^{-1}$ measured by D'Anna et al.³² at $298 \pm 2 \text{ K}$ relative to 1-butene, whereas our rate constant for the reaction of OH radicals with 4,4-dimethyl-1-pentene ($2.41 \times 10^{-11} \text{ molecule}^{-1} \text{ s}^{-1}$; average of the two values relative to methacrolein and 1-octene) is the first reported for this alkene. Our measured rate constant for 4,4-dimethyl-1-pentene is consistent with literature data for reactions of OH radicals with 1-alkenes^{5,23} and with the value of $2.8 \times 10^{-11} \text{ molecule}^{-1} \text{ s}^{-1}$ calculated using the structure–reactivity estimation method of Kwok and Atkinson.¹² The observation that the rate constant for OH + 4,4-dimethyl-1-pentene is slightly lower than predicted and lower than the corresponding rate constants for propene and the C₄–C₇ 1-alkenes^{5,23} suggests that this may be due to steric effects, with the $(\text{CH}_3)_3\text{C}$ group screening the C=C bond to some extent (see, for example, ref 33 for steric effects in the reactions of O₃ with alkenes).

3,3-Dimethylbutanal was the major product observed and quantified from OH + 4,4-dimethyl-1-pentene, with a formation yield of $59 \pm 6\%$. As noted above, many of the product peaks observed in the GC-FID and GC-MS analyses of the OH + 4,4-dimethyl-1-pentene reaction were second-generation products from OH + 3,3-dimethylbutanal (for example, acetone, *tert*-butyl nitrite and *tert*-butyl nitrate; see Scheme 5). The first-generation products observed from OH + 4,4-dimethyl-1-pentene were, in addition to 3,3-dimethylbutanal, acrolein ($2.7 \pm 0.5\%$), a MW 112 carbonyl attributed to 4,4-dimethyl-2-pentenal [$(\text{CH}_3)_3\text{CCH}=\text{CHCHO}$] ($3.4 \pm 0.6\%$); and products of MW 146, 177, and 193. On the basis of the expected reaction schemes shown in Schemes 3 and 4 for OH radical addition to the terminal and internal carbon atoms of the C=C bond, respectively, the products of MW 146, 177, and 193 can be attributed to the dihydroxycarbonyl $\text{HOCH}_2\text{C}(\text{CH}_3)_2\text{CH}_2\text{C}(\text{O})\text{CH}_2\text{OH}$, the hydroxynitrates $(\text{CH}_3)_3\text{CCH}_2\text{CH}(\text{OH})\text{CH}_2\text{ONO}_2$ and/or $(\text{CH}_3)_3\text{CCH}_2\text{CH}(\text{ONO}_2)\text{CH}_2\text{OH}$, and the dihydroxynitrate $\text{O}_2\text{NOCH}_2\text{C}(\text{CH}_3)_2\text{CH}_2\text{CH}(\text{OH})\text{CH}_2\text{OH}$, respectively. The MW 146 dihydroxycarbonyl and MW 193 dihydroxynitrate are expected to be formed only after OH radical addition at the terminal (1-position) carbon atom and subsequent isomerization of the resulting intermediate hydroxyalkoxy radical $(\text{CH}_3)_3\text{CCH}_2\text{CH}(\text{O}^\bullet)\text{CH}_2\text{OH}$. For both $(\text{CH}_3)_3\text{CCH}_2\text{CH}(\text{O}^\bullet)\text{CH}_2\text{OH}$ and $(\text{CH}_3)_3\text{CCH}_2\text{CH}(\text{OH})\text{CH}_2\text{O}^\bullet$, reaction with O₂ to form 1,2-hydroxycarbonyls is expected to be minor or negligible compared to decomposition and/or isomerization,³⁴ and the O₂ reactions have therefore been omitted from Schemes 3 and 4. The products we observe are therefore in accord with expectations³⁴ of the products formed after initial OH radical addition to 4,4-dimethyl-1-pentene.

The OH radical can also react by H-atom abstraction from the 3-position CH₂ group and from the three CH₃ groups, and reaction schemes based on our knowledge of the subsequent reactions are shown in Schemes 1 and 2, respectively. In Scheme 2, it is expected that decomposition of the [•]OCH₂C(CH₃)₂-CH₂CH=CH₂ radical will dominate over its reaction with O₂, by a factor of ~6 at 298 K and atmospheric pressure of air.³⁴ Hence, the products expected after H-atom abstraction from the three CH₃ groups are mainly formaldehyde, acrolein, and acetone (Scheme 2). H-atom abstraction from the 3-position CH₂ group is predicted (Scheme 1) to lead to acrolein + acetone + methyl radical (with the methyl radical reacting to form HCHO, CH₃ONO, and CH₃ONO₂ under our conditions²²) and/or 4,4-dimethyl-2-pentenal. Acetone is also a second-generation product of OH + 3,3-dimethylbutanal (Scheme 5), and hence its formation yield from OH + 4,4-dimethyl-1-pentene could not be quantified. However, our acrolein and 4,4-dimethyl-2-pentenal formation yields of 2.7 ± 0.5% and 3.4 ± 0.6%, respectively, indicate that H-atom abstraction accounts for 6.1 ± 0.8%, neglecting any minor formation of CH₂=CHCH₂C(CH₃)₂CHO (see Scheme 2). H-atom abstraction from the 3-position CH₂ group accounts for ≥3.4 ± 0.6% of the overall reaction, based on the yield of 4,4-dimethyl-2-pentenal. The Kwok and Atkinson estimation method¹² predicts that at 298 K H-atom abstraction from the three equivalent CH₃ groups and from the 3-position CH₂ group account for 1.8 and 4.1% of the overall reaction, respectively, with partial rate constants of 5.0 × 10⁻¹³ and 1.15 × 10⁻¹² cm³ molecule⁻¹ s⁻¹, respectively.¹² The predicted¹² total partial rate constant for H-atom abstraction of 1.65 × 10⁻¹² cm³ molecule⁻¹ s⁻¹ is in excellent agreement with our value of (1.47 ± 0.25) × 10⁻¹² cm³ molecule⁻¹ s⁻¹ derived from the measured overall rate constant [(2.41 ± 0.25) × 10⁻¹¹ cm³ molecule⁻¹ s⁻¹] and the fraction of the reaction proceeding by H-atom abstraction. This agreement suggests that this structure–reactivity estimation method¹² can be used to calculate the importance of H-atom abstraction in the reactions of OH radicals with other acyclic alkenes for which data are not presently available.

Acknowledgment. The authors gratefully thank the National Science Foundation (Grant No. ATM-0234586) for supporting this research. Although this research has been supported by this agency, it has not been reviewed by the agency and no official endorsement should be inferred. Dr. Douglas Lane (Environment Canada) is thanked for supplying the ground XAD used to coat the denuder.

References and Notes

(1) Guenther, A.; Hewitt, C. N.; Erickson, D.; Fall, R.; Geron, C.; Graedel, T.; Harley, P.; Klinger, L.; Lerdau, M.; McKay, W. A.; Pierce,

- T.; Scholes, B.; Steinbrecher, R.; Tallamraju, R.; Taylor, J.; Zimmerman, P. *J. Geophys. Res.* **1995**, *100*, 8873.
 (2) Zielinska, B.; Sagebiel, J. C.; Harshfield, G.; Gertler, A. W.; Pierson, W. R. *Atmos. Environ.* **1996**, *30*, 2269.
 (3) Calvert, J. G.; Atkinson, R.; Kerr, J. A.; Madronich, S.; Moortgat, G. K.; Wallington, T. J.; Yarwood, G. *The Mechanisms of Atmospheric Oxidation of the Alkenes*; Oxford University Press: New York, 2000.
 (4) Atkinson, R. *J. Phys. Chem. Ref. Data* **1997**, *26*, 215.
 (5) Atkinson, R.; Arey, J. *Chem. Rev.* **2003**, *103*, 4605.
 (6) Ohta, T. *Int. J. Chem. Kinet.* **1984**, *16*, 1495.
 (7) Atkinson, R.; Tuazon, E. C.; Carter, W. P. L. *Int. J. Chem. Kinet.* **1985**, *17*, 725.
 (8) Atkinson, R.; Tuazon, E. C.; Aschmann, S. M. *Int. J. Chem. Kinet.* **1998**, *30*, 577.
 (9) Peeters, J.; Vandenberk, S.; Piessens, E.; Pultau, V. *Chemosphere* **1999**, *38*, 1189.
 (10) Tuazon, E. C.; Aschmann, S. M.; Nguyen, M. V.; Atkinson, R. *Int. J. Chem. Kinet.* **2003**, *35*, 415.
 (11) Jenkin, M. E.; Sulbaek Andersen, M. P.; Hurley, M. D.; Wallington, T. J.; Taketani, F.; Matsumi, Y. *Phys. Chem. Chem. Phys.* **2005**, *7*, 1194.
 (12) Kwok, E. S. C.; Atkinson, R. *Atmos. Environ.* **1995**, *29*, 1685.
 (13) Kwok, E. S. C.; Atkinson, R.; Arey, J. *Environ. Sci. Technol.* **1996**, *30*, 1048.
 (14) Aschmann, S. M.; Atkinson, R.; Arey, J. *J. Geophys. Res.* **2002**, *107*, DOI: 10.1029/2001JD001098.
 (15) Nishino, N.; Arey, J.; Atkinson, R. *J. Phys. Chem. A* **2009**, *113*, 852.
 (16) Reisen, F.; Aschmann, S. M.; Atkinson, R.; Arey, J. *Environ. Sci. Technol.* **2003**, *37*, 4664.
 (17) Peters, A. J.; Lane, D. A.; Gundel, L. A.; Northcott, G. L.; Jones, K. C. *Environ. Sci. Technol.* **2000**, *34*, 5001.
 (18) Arey, J.; Obermeyer, G.; Aschmann, S. M.; Chattopadhyay, S.; Cusick, R. D.; Atkinson, R. *Environ. Sci. Technol.* **2009**, *43*, 683.
 (19) Obermeyer, G.; Aschmann, S. M.; Atkinson, R.; Arey, J. *Atmos. Environ.* **2009**, *43*, 3736.
 (20) Scanlon, J. T.; Willis, D. E. *J. Chromat. Sci.* **1985**, *23*, 333.
 (21) Taylor, W. D.; Allston, T. D.; Moscato, M. J.; Fazekas, G. B.; Kozlowski, R.; Takacs, G. A. *Int. J. Chem. Kinet.* **1980**, *12*, 231.
 (22) Atkinson, R.; Baulch, D. L.; Cox, R. A.; Crowley, J. N.; Hampson, R. F.; Hynes, R. G.; Jenkin, M. E.; Rossi, M. J.; Troe, J. *Atmos. Chem. Phys.* **2006**, *6*, 3625.
 (23) Aschmann, S. M.; Atkinson, R. *Phys. Chem. Chem. Phys.* **2008**, *10*, 4159.
 (24) Wallington, T. J.; Andino, J. M.; Potts, A. R.; Nielsen, O. J. *Int. J. Chem. Kinet.* **1992**, *24*, 649.
 (25) Atkinson, R.; Aschmann, S. M.; Carter, W. P. L.; Winer, A. M.; Pitts, J. N., Jr. *J. Phys. Chem.* **1982**, *86*, 4563.
 (26) Atkinson, R. *J. Phys. Chem. Ref. Data* **1994**, *Monograph 2*, 1.
 (27) Woidich, S.; Froescheis, O.; Luxenhofer, O.; Ballschmiter, K. *Fresenius J. Anal. Chem.* **1999**, *364*, 91.
 (28) Muthuramu, K.; Shepson, P. B.; O'Brien, J. M. *Environ. Sci. Technol.* **1993**, *27*, 1117.
 (29) Atkinson, R. *Atmospheric Oxidation in Handbook of Property Estimation Methods for Chemicals, Environmental and Health Sciences*; Boethling, R. S., Mackay, D., Eds.; Lewis Publishers: Boca Raton, FL, 2000; pp 335–354.
 (30) O'Brien, J. M.; Czuba, E.; Hastie, D. R.; Francisco, J. S.; Shepson, P. B. *J. Phys. Chem. A* **1998**, *102*, 8903.
 (31) Matsunaga, A.; Ziemann, P. J. *J. Phys. Chem. A* **2009**, *113*, 599.
 (32) D'Anna, B.; Andresen, Ø.; Gefen, Z.; Nielsen, C. J. *Phys. Chem. Chem. Phys.* **2001**, *3*, 3057.
 (33) McGillen, M. R.; Carey, T. J.; Archibald, A. T.; Wenger, J. C.; Shallcross, D. E.; Percival, C. J. *Phys. Chem. Chem. Phys.* **2008**, *10*, 1757.
 (34) Atkinson, R. *Atmos. Environ.* **2007**, *41*, 8468.

JP101893G